Proceedings of the SEM Annual Conference
June 1-4, 2009 Albuquerque New Mexico USA

3D and 2D High Speed Image Correlation for Dynamic Testing

Tim Schmidt and John Tyson, Trilion Quality Systems, 500 Davis Drive, Suite 200, Plymouth Meeting, PA 19462

ABSTRACT

Various practical aspects of high rate full-field measurements are presented together with the associated experimental results. Applications include split Hopkinson pressure bar (SHPB) tension and torsion tests as well as four point bend for dynamic fracture, and large-area outdoor point target tracking.

3D and 2D high speed image correlation are explicitly compared on identical aluminum flat tension SHPB specimens. It is found that 2D provides accurate results at various working distances, even when the camera is off-axis by approximately 10 degrees.

Other experimental findings of interest include double necking in an as-forged tantalum tension SHPB specimen, shear failure of a commercially pure zirconium compression SHPB specimen, and torsion test results on polycarbonate.

Zirconium-based bulk metallic glass (BMG) and other composite materials are tested on the modified SHPB in 4 point bend. The Shimadzu HPV-1 camera is used to acquire notch opening displacements at 1 million fps. Full-field 2D data is acquired at 500,000 fps with the Shimadzu, and 3D displacements and surface strains are acquired with Photron SA1.1 cameras at 100,000 fps. The goal is to better understand dynamic failure mechanisms of these new materials.

A large area calibration method is used together with 3D point tracking software to obtain operating deflection shape data on an 18 meter diameter x 28 meter tall water tank as it is being filled. The calibration method supports automatic frame by frame re-calibration to compensate for relative camera movements when required. There is no upper limit on the size of the field of view.

High speed and ultra high speed image correlation are extremely well-established tools now. New insights can be gained by combining the latest camera technology with excellent and innovative experimental technique.

INTRODUCTION

3D image correlation has been extensively developed and validated for measurements on tension, torsion and compression split Hopkinson bar tests, and is being used regularly for this and other dynamic applications [1-5]. Subsequently, it was considered desirable to also assess the feasibility of using a single high speed camera to measure full-field strains on flat tension specimens. The benefits of this approach would be lower cost and faster setup compared to the now-proven 3D method.

EXPERIMENTAL CONSIDERATIONS AND SETUP FOR 2D ASSESSMENT

The strategy was to perform two 2D tests on a type of specimen that had previously been characterized using the Aramis 3D image correlation system, and compare the strain time histories and necking diagrams. One test was done with a 105 mm focal lens and a working distance of 32”, and the other was done using a 55 mm lens with a working distance of 10”. This was done because errors in 2D image correlation from out-of-plane movement, including from the Poisson effect, are known to increase as the working distance is decreased (unless a telecentric lens is used). Varying the working distance would give a first quick look for possible errors.

Figure 1 is a comparison of two 2D tests to a prior 3D test on what were thought to be identical 2024-T351 aluminum specimens. It can be seen that, although the two 2D results are identical except for the final necking, there is a significant discrepancy from the prior 3D result. To further investigate the feasibility of 2D image correlation on flat tension specimens, 2D projects were created from the left and right cameras of a prior 3D project for an epoxy material that was recorded at 180,000 frames per second. The results are shown in Figure 2. It can be seen that, despite the differences in view angle between the left and right cameras (each about 15 degrees off-axis), the results were virtually identical until the very end of the test. Slightly different views of the epoxy tearing and moving out-of-plane explain the difference in final peak values. The 2D projects from the left and right cameras for the earlier specimen (Figure 3) matched even more closely, through the final necking.

It was found that although the specimens used for the 2D study were cut from a 0.5" plate of Al 2024-T351, the 2D specimens were different; they were cut from a 0.125" plate of Al 2024-T3 temper. This was part of a broader study to characterize aluminum alloys for dynamic loading applications [6] The 2D results were further validated by comparison to the strain time histories from the elastic waves (Figure 4). It can be seen that, as was the case for dozens of 3D validation tests, the image correlation strains match the elastic wave strains until the onset of necking, when the image correlation then indicates the true local strain in the necking region. Figure 5 and Figure 6 are the necking diagram and a full-field result from a 2D test of the 2024-T351 specimen, which are typical Aramis outputs for such a test.

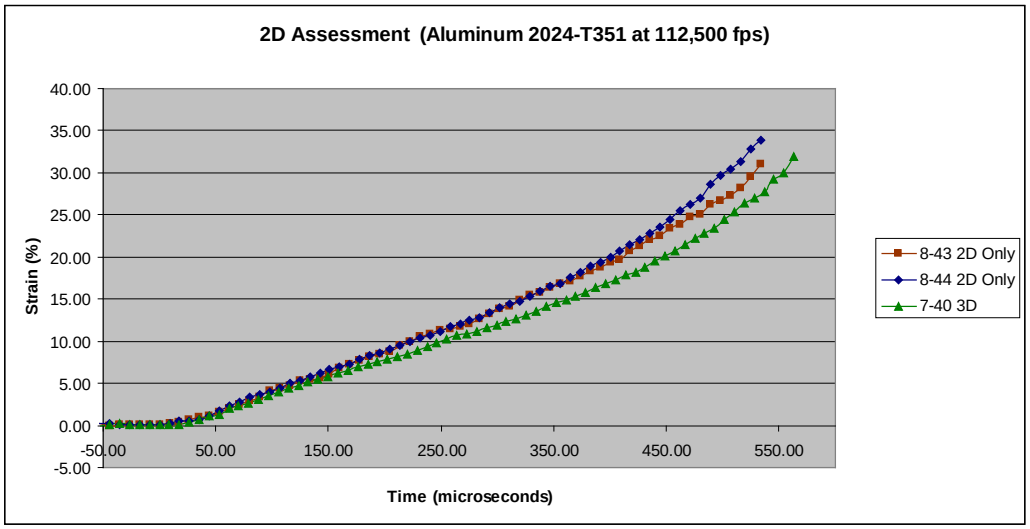

Figure 1: Comparison of two 2D tests to a prior 3D test on what were thought to be identical Al 2024-T351 specimens. It can be seen that, although the two 2D results are identical except for the final necking, there is a significant discrepancy from the prior 3D result.

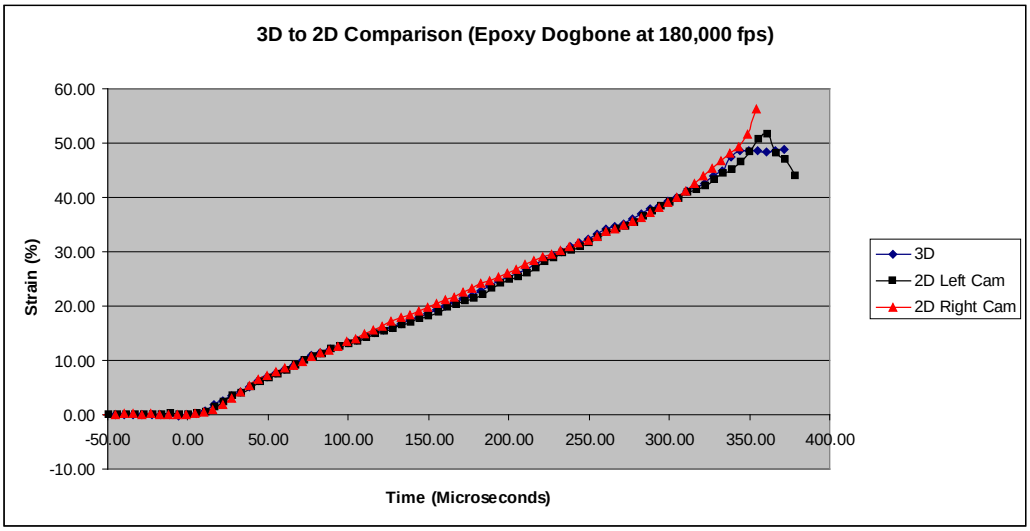

Figure 2: To further investigate the feasibility of 2D image correlation on flat tension specimens, 2D projects were created from the left and right cameras of a prior 3D project. It can be seen that, despite the differences in view angle between the left and right cameras, the results were virtually identical until the very end of the test. Slightly different views of the epoxy tearing and moving out-of-plane explain the difference in final peak values.

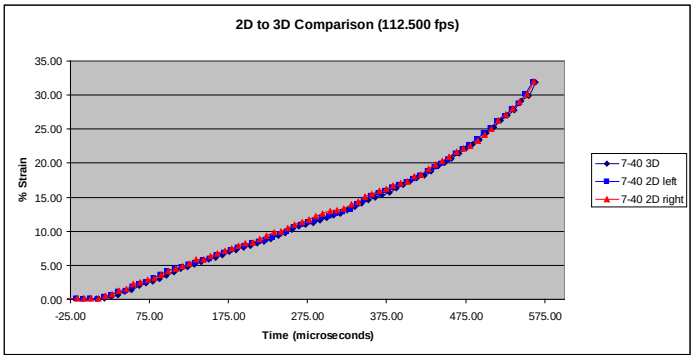

Figure 3: The 2D projects from the left and right cameras for the earlier specimen matched even more closely, through the final necking.

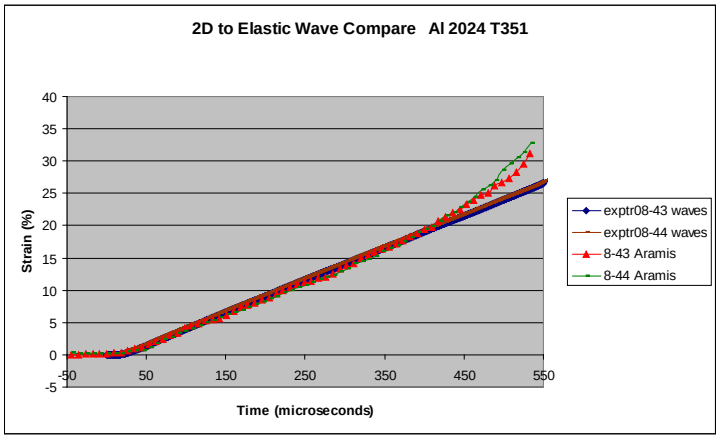

Figure 4: It was found that the specimens used for the 2D study were in fact cut from a different plate, which was 0.125" thick with 2024-T351 temper. The 2D results were further validated by comparison to the strain time histories from the elastic waves. It can be seen that, as was the case for dozens of 3D validation tests, the Aramis strains match the elastic wave strains until the onset of necking, when Aramis then indicates the true local strain in the necking region.

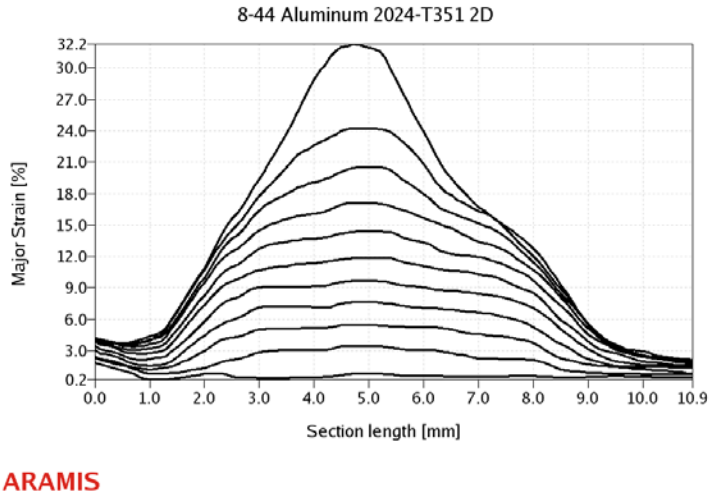

Figure 5: Necking diagram from the 2D test with 10" working distance, showing the progression of strain profile along the specimen length at 44 microsecond intervals (every 5th frame of 112,500 fps recording is shown for clarity).

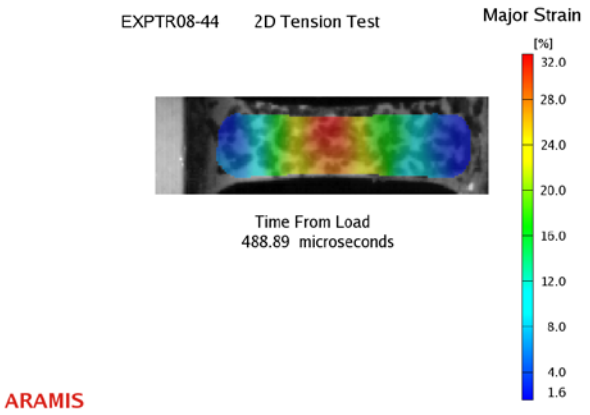

Figure 6: Full-field strain overlay for 2D image correlation test of 2024-T351 specimen indicating necking region shortly before fracture.

Having established a comfort level with 2D image correlation for the split Hopkinson Bar using typical digital high speed cameras, it was natural to proceed to assess the use of more specialized cameras as well, which would provide various benefits due to their unique features. The Shimadzu HPV camera, for example, enables recording up to 100 frames at up to 1 million frames per second with a constant resolution of 312 x 260 pixels, onto a single sensor with a single optical path, using a special IS-CCD sensor. Higher frame rates are necessary when testing brittle materials on the Hopkinson Bar, for which the load time will be at least an order of magnitude lower than for ductile metals, in the tens of microseconds at best, instead of hundreds of microseconds or more. The single sensor and optical path eliminates any concerns about optical aberrations or false strains and displacements due to optical path differences between the reference (0 strain and displacement) and test images. Although CMOS cameras such as the Phantoms and Photrons gain significant speed for a given resolution every few years or so, they do not approach the Shimadzu, and are better suited for applications that can take advantage of their higher initial resolution at lower frame rates, and/or the vastly higher number of frames that can be captured, which ranges from about 5,000 to 50,000 or more depending on the resolution. On CMOS cameras, the resolution decreases as frame rate increases, so the user must make a compromise between temporal and spatial resolution. To provide a comparison to the Shimadzu capability, it is noted that currently available CMOS cameras are capable of from 30,000 to 67,000 frames per second at 256 x 256 pixel resolution.

The Shimadzu HPV-1 was tested on a modified split Hopkinson Bar set up for dynamic 4 point bend tests. The goal was to make an initial assessment of the applicability and potential benefits of using image correlation to continue studying the high rate behavior of Zr-based bulk metallic glass (BMG) [7-8] and other materials. Bulk metallic glasses are amorphous (non-crystalline) materials that can be stronger than metals and tougher than ceramics. However, they can fail suddenly in tension, limiting their usefulness for certain critical applications. Therefore, materials researchers are attempting to produce metal matrix composites based on BMGs. It is necessary to understand the dynamic failure mechanism of these new materials, and to also study conventional materials in a similar manner.

Figure 7 shows the notch opening displacements for an aluminum laminate specimen subjected to dynamic 4 point bending. A clean time history was obtained, accurately recording the notch opening until and after fracture occurred about 60 microseconds after impact. Such crack opening graphs can be directly obtained using a user-definable point to point extensometer between facets (subsets) that are straddling the notch or crack of interest. Because the material surrounding the crack tends to move as a rigid body, the result is typically not highly sensitive to the original length of the extensometer. However, it is good experimental practice to make a few extensometers of various lengths and explicitly check for repeatability. Figure 8 is the full-field transverse strain result captured 10 microseconds after impact on a second aluminum laminate specimen, indicating a tensile strain away from the notch at the eventual failure location.

3D image correlation was used on the modified SHPB with Photron SA1.1 cameras for composite specimens. Figure 9 is the transverse strain (in the direction of the notch) overlay 190 microseconds after load initiation for an S2 composite in high rate 4 point bend. There is a second tensile strain region beyond the usual one at the notch tip. The strains perpendicular to the notch direction at various locations of interest are fully quantified over time in Figure 10. The extra effort to set up the 3D system was made in order to be able to analyze the out-of-plane displacements, which are shown in Figure 11. It is expected that these can provide further insight into the failure mechanism as well as provide information about the test setup alignment and verification of boundary conditions.

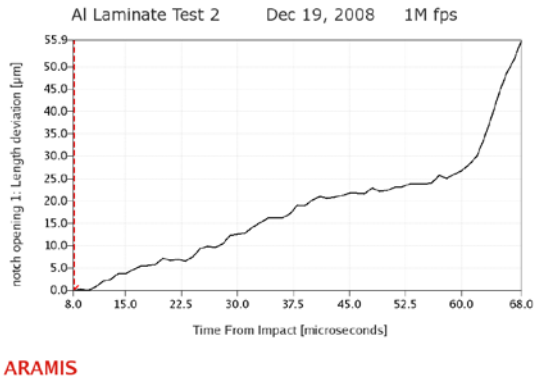

Figure 7: Notch opening time history obtained at 1 million frames per second with the Shimadzu HPV1 camera.

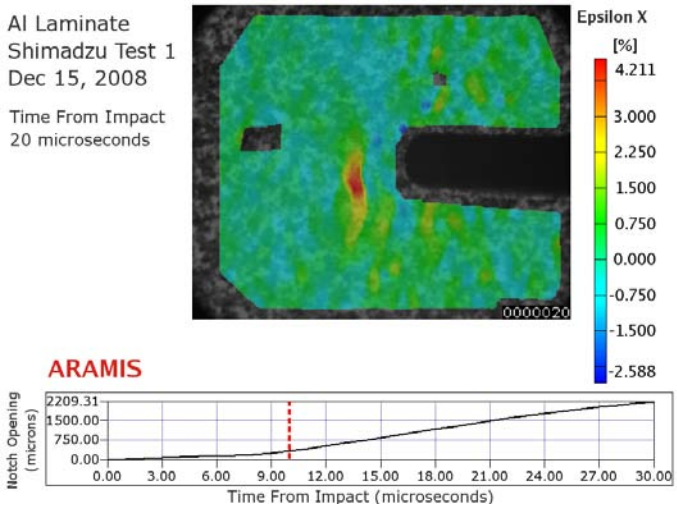

Figure 8: Full-field transverse strain result captured 10 microseconds after impact with the Shimadzu HPV-1 camera.

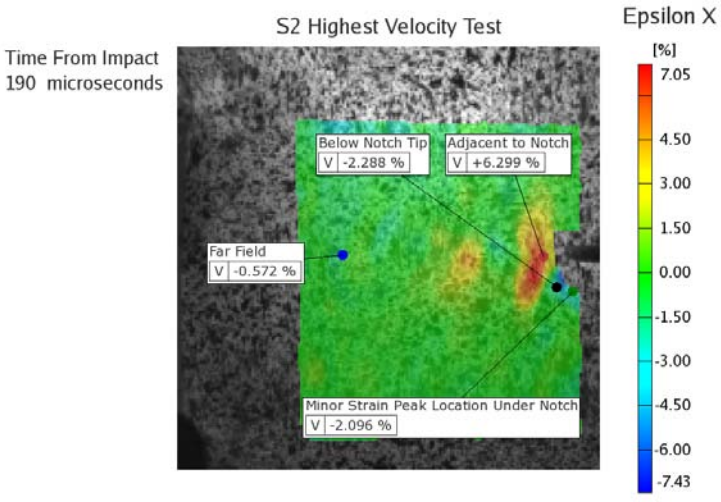

Figure 9: Transverse strain overlay 190 microseconds after load initiation for an S2 composite in high rate 4 point bend, captured with Photron SA1.1 cameras at 100,000 fps. There is a second tensile strain region beyond the usual one at the notch tip.

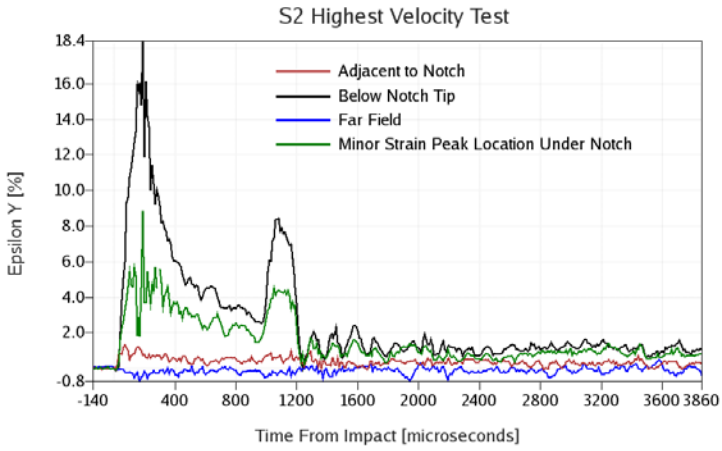

Figure 10: Strain time history for several points of interest, extending through numerous reflections of the elastic waves in the incident bar.

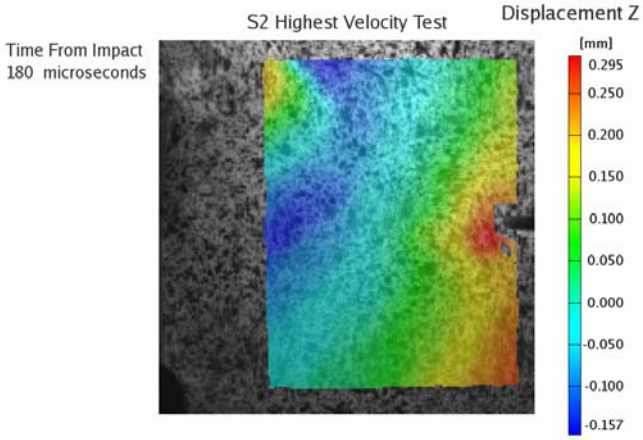

Figure 11: Out-of-plane displacement analysis may provide further insight into the specimen behavior.

The improved performance of the Photron SA1.1 cameras compared to the APX-RS model ease the experimental setup to capture a torsion split Hopkinson bar test on polycarbonate. The specimen had an unfavorable geometry, with the 0.1" gage deeply recessed from the spool O.D. It was therefore necessary to align the camera stereo pair vertically, to eliminate the perspective change between the two cameras and image the entire gage. As shown in Figure 12, data was successfully acquired across the entire gage, using 256 x 128 pixels at 125,000 fps. The overlaid section line itself provides a measure of the shear angle, since it deformed to follow the facets that were used to define it in the reference image. Figure 13 confirms that the entire time history was also fully captured; in fact, the spool has unwound due to the reflected wave, and is shearing in the opposite direction. Strictly speaking, a Hopkinson Bar test is over once the first elastic wave has transited through the gage, but unless a momentum trap is used, the specimen will undergo numerous repeat loadings due to wave reflections. Therefore, the final condition of the recovered specimen does not accurately represent the post-test condition. Nevertheless, it was pleasing to find that the standard patterning technique of spray paint dots was adequate even on translucent plastic, with no evidence of flaking or micro-cracking.

The Photron APX RS cameras and equivalents such as the Phantom v7 series remain adequate for numerous tests including the Split Hopkinson Pressure Bar (SHPB). Figure 14 shows several interesting results that were obtained on as-forged tantalum specimens. Both double necking and off-center necking were captured. Of even greater importance was the shear failure of a commercially pure zirconium specimen during a compression test, the principal strain II overlay shortly before ultimate failure is shown in Figure 15.

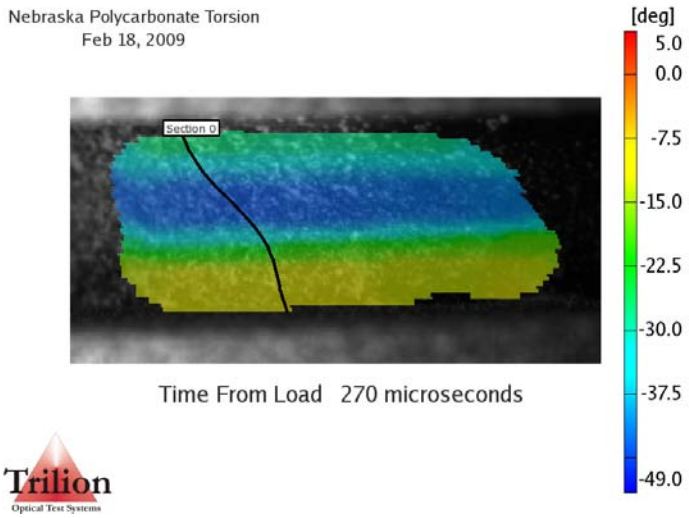

Figure 12: Full-field overlay of principal strain for polycarbonate torsion test. Note that the data occupies the entire width of the gage.

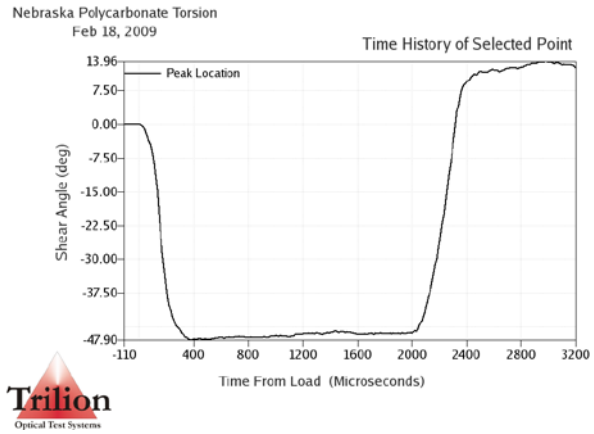

Figure 13: Principal strain time history for a point within the band of peak strain for a polycarbonate torsion test. Data was acquired well past the end of the first elastic wave; note that the spool has unwound due to the reflected wave.

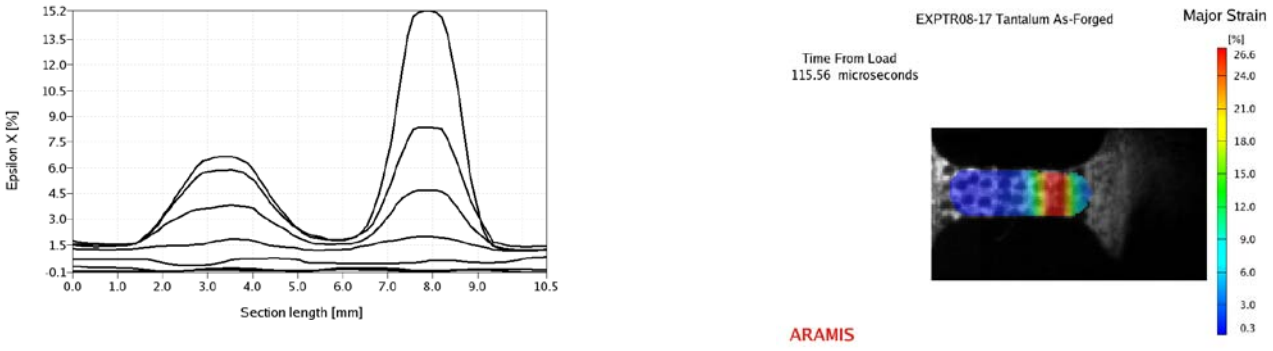

Figure 14: ARAMIS waterfall plot showing double necking that occurred on an as-forged tantalum tension test, and full-field color plot of off-center necking on a different as-forged tantalum specimen.

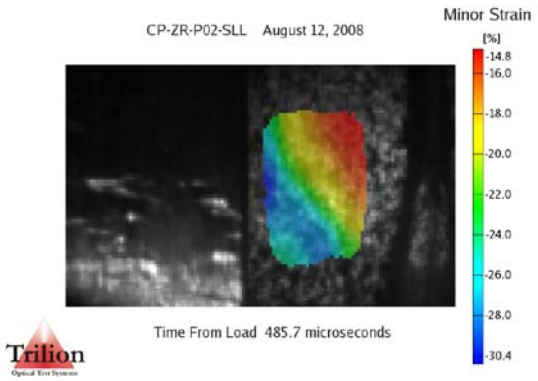

Figure 15: Principal strain II overlay for a SHPB compression test on a commercially pure zirconium specimen that failed in shear.

Brittle material such as ceramics or carbon fiber composites require much higher frame rates than CMOS cameras can provide. High spatial resolution may also be critical for applications such as delamination of composites, or to resolve strains near crack tips and between multiple propagating cracks. These situations are best addressed with an ultra high speed camera such as the Cordin 550.

As shown in Figure 16, the Cordin 550 rotating mirror camera has an extremely complex optical path. A field lens relays the image from the front objective through an aperture into a series of beamsplitters. The image is eventually fed by the five-sided rotating mirror into individual CCD sensors that are arranged in semi-circular banks of 8. The differences in the optical paths between the sensors are known to cause significant false strains and displacements. It may still be possible to perform image correlation on all of the frames sequentially in the usual manner, using the first frame as the reference for all that follow. A correction would need to be applied to each frame to subtract out the false strains and displacements, perhaps using a look-up table approach. However, as pointed out by Kirugulige [9-10], there is a simpler method, whereby a set of reference images is acquired for all sensors, and then each test image is referenced back to the same sensor. This eliminates the errors from the optical path differences, which is extremely important because in practice, two further complications would arise with efforts to subtract out errors from optical path differences for each frame. Due to the nature of the triggering of the Cordin camera, the first frame might occur on any of the sensors, meaning that at least 16 different sets of corrections would have to be prepared. Furthermore, any change in the internal alignment of the camera would necessitate making a complete new set of corrections.

Therefore, a demonstration measurement was made using the self-referencing method, as shown in Figure 17. For these experimental strain levels, no noise is evident at all. As should be expected, detailed noise floor maps are being generated and repeatability studies are being made so that full-field strain and displacement accuracies can be stated with confidence, particularly to support measurements on brittle materials with much lower ultimate strains. The particular electric drive model used was limited to 16 frames at 300,000 fps, but the method would work equally well on gas turbine Cordin models which are available with up to 62 imaging sensors at up to 4 million fps.

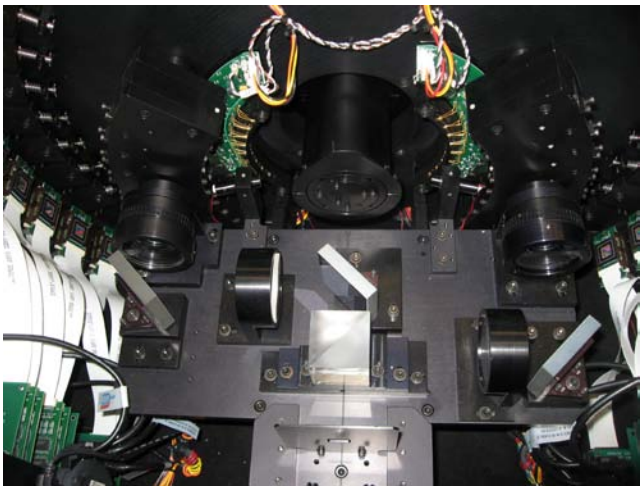

Figure 16: Partial view of the Cordin 550 optical paths. The field lens and objective are out of sight below the bottom of the image. Three CCDs are visible at the middle left, and one at the middle right. The individual final relay lenses for each CCD are contained within the semi-circular black enclosure.

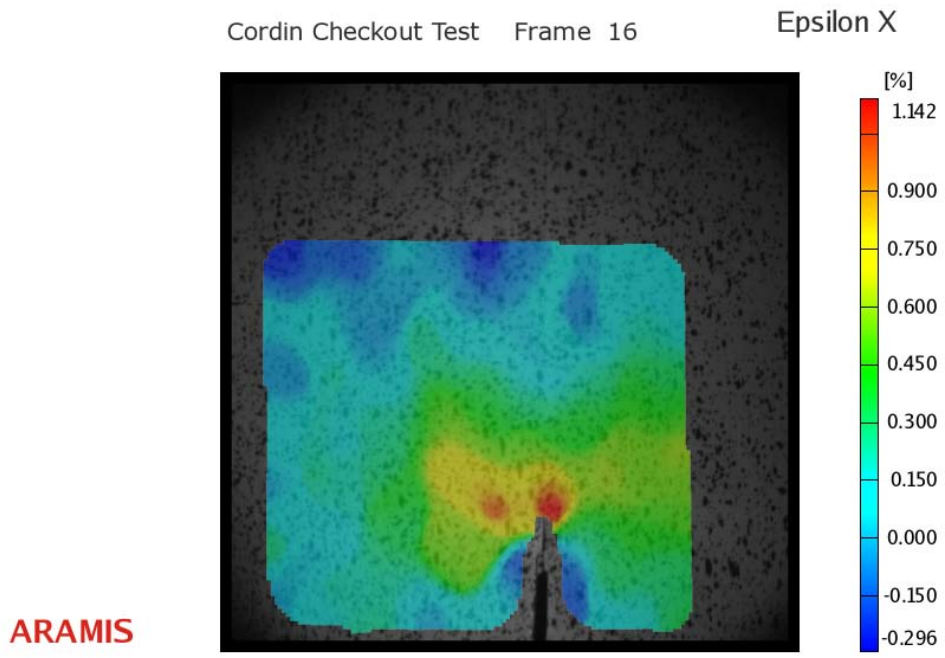

Figure 17: Full-field transverse strain result on a notched specimen obtained with a Cordin 550 camera that has 16 installed CCD sensors with an electric drive spinning the five-sided mirror.

There are more and more applications that require extremely large fields of view at relatively slow frame rates, typically from 50 to 1,000 fps. Cameras with the largest possible number of pixels in the transverse direction are desirable for these projects, in order to reduce the required size of the dot targets to be tracked and to maximize spatial resolution on small regions of interest within the overall field of view. Figure 18 is an example of a large area application that provided some illustrative challenges. A consulting engineer was asked to strain gauge an 18 meter diameter x 28 meter tall water tank that was observed to be buckling somewhat during rapid filling. In order to determine the likely peak stress locations, it was desirable to determine the operating deflection shapes (ODS) of the tank. The PONTOS point tracking system was used with 4 Megapixel cameras at 50 fps, together with a large area calibration method. Figure 19 shows the stereo camera setup in the field, where the ambient temperature was -35 degrees Celsius, supplemented by strong gusting winds. The cameras were mounted on separate tripods that were embedded in snow-banks approximately 12 meters apart. It was then discovered that the cameras were rated for operation in temperatures from 0 to 40 degrees Celsius. In order to simulate these conditions, large kerosene heaters were placed to warm up the cameras. They were turned off and away from the cameras for brief bursts of data acquisition, to prevent adverse lensing effects fro the thermal currents. This proved successful, although in the future temperature controlled enclosures would be used. Figure 20 shows the displacement time histories for numerous dot targets on the tank. It can clearly be seen that there are groups of points moving in a fixed phase relationship. The ODS is more clearly visible in Figure 21, where displacement vectors reveal the dominant diametrical bending shape of the tank. It was found that the peak displacement locations, clearly visible in the color map of Figure 22, shifted upwards as the tank filled, staying just above the water level.

The cameras were calibrated using the measurement targets on the test object itself. In the bundle adjustment used to determine the photogrammetric interior and exterior orientations, only one image from the stereo pair is needed to determine the camera positions relative to each other. Therefore, the system can be automatically recalibrated frame by frame when needed in the event of ground shake, as can happen during certain types of ballistic or ground impact tests [11]. For swing tests, the calibration target array has been mounted on a wall that remains in view behind the test article throughout the test [12].

There is no upper limit on the size of the field of view that can be measured; the operational deflection shapes of full-scale wind turbines have been successfully recorded [13].

Figure 18: Six-inch dot targets and coded targets applied to 18 meter diameter x 23 meter tall water tank in order to determine the operating deflection shapes at various fill heights. Note the engineer at bottom right for scale.

Figure 19: The stereo camera setup in the field, with kerosene heaters to enable camera operation far below their normal rated temperature. Temperature-controlled enclosures will be used in the future.

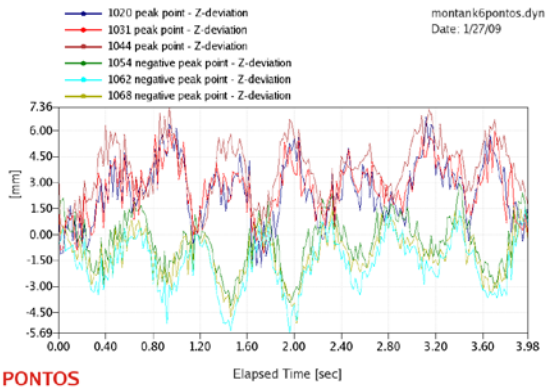

Figure 20: Time histories of the peak displacement points, with very consistent phase relationships.

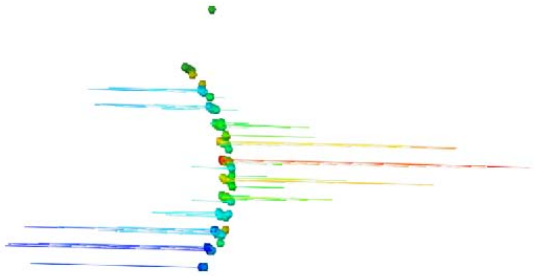

Figure 21: Side view of the resultant displacement vectors, which were used to determine the dominant diametrical bending mode.

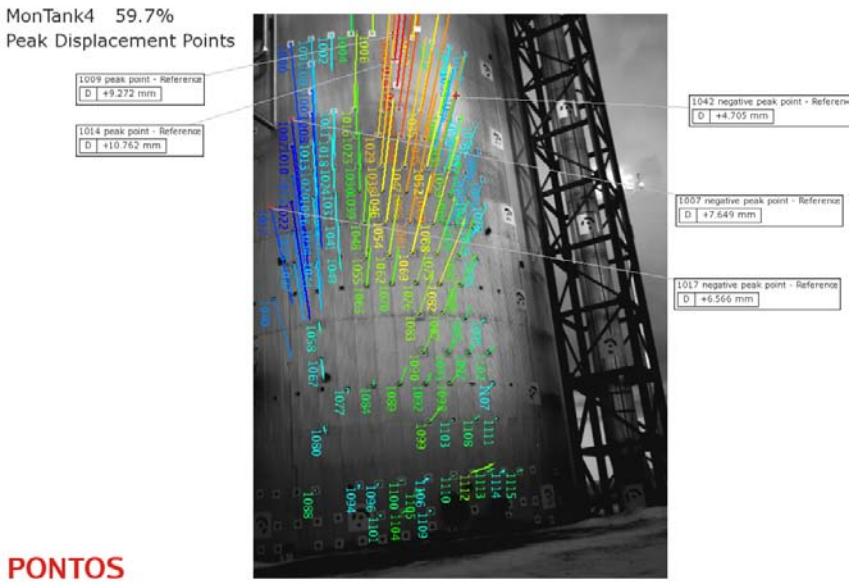

Figure 22: Peak locations were found to shift upwards as the water level rose.

CONCLUSIONS

It was found that 2D image correlation can accurately capture the full-field strains and necking for tension split Hopkinson Bar tests, even when the single high speed camera is not perfectly aligned to the specimen.

The Shimadzu HPV1 camera was used to acquire notch and crack opening displacements and full-field displacement and strain results at up to 1 million frames per second. 3D image correlation was also successfully performed on the modified SHPB 4 point bend test on various composite and bulk metallic glass specimens in order to better understand their dynamic failure.

Full-field strains at a crack tip were readily acquired using a Cordin 550 rotating mirror camera. The particular electric drive model used was limited to 16 frames at 300,000 fps, but the method would work equally well on gas turbine Cordin models which are available with up to 62 imaging sensors at up to 4,000,000 fps.

This paper does not advocate the use of any specific camera over another. The goal is to encourage taking full advantage of continually improving high speed camera and image correlation methodology to gain new insight into dynamic processes.

ACKNOWLEDGMENTS

Jeremy Seidt of THE Ohio State University conducted the initial 3D tests on 2024 aluminum, and provided the 2D dog-bone specimens that were also used for the 2D to 3D comparisons. The work was performed in Amos Gilat's laboratory.

Dr Vikas Prakash and Dr. John Lewandowski supported the four point bend testing on the modified split Hopkinson bar apparatus at Case Western Reserve University. George Sunny conducted all of the modified SHPB experiments. Their interest is greatly appreciated.

Todd Rumbaugh, Manager Ultra High Speed Cameras, Hadland Imaging LLC, provided and excellently supported the Shimadzu HPV1 camera.

Dr. Mehrdad Negahban coordinated the polycarbonate torsion tests at the University of Nebraska – Lincoln. Jason Vogeler and his advisor Dr. Ruqiang Feng conducted the experiments.

The as-forged tantalum and commercially pure zirconium tests were done as part of the US Force SBIR Phase II Contract FA8651-06-C-0123, "Revolutionary Materials Research Technology For High-Strain Rate Ordnance Research". The technical sponsor was Dr. Joel House and the technical monitor was Mr. Philip Flater.

Thanks to Dr. Tony Waas, Director of the Composite Structures Laboratory at the University of Michigan – Ann Arbor, for allowing use of the Cordin 550 camera results. Mark Pankow prepared the specimens and obtained the test images.

REFERENCES

1) Schmidt, Tyson, Revilock et al, Performance Verification of 3D Image Correlation Using Digital High-Speed Cameras, Proceedings of the SEM Annual Conference and Exposition, Portland, OR, June 7-9, 2005.

2) Schmidt, Tyson, Galanulis, Revilock and Melis, Full-field dynamic deformation and strain measurements using high-speed digital cameras, Proceedings of the SPIE 26th International Congress on High-Speed Photography and Photonics, Alexandria, VA, Sept 19, 2004.

3) Gilat, Schmidt and Tyson, Full-Field Strain Measurement During a Tensile Split Hopkinson Bar Experiment, Presented at the SEM Annual Conference and Exposition, St. Louis, June 6, 2006.

4) Schmidt, Gilat, Tyson and Walker, Further Development and Validation of Full-Field Strain Measurements for Hopkinson Bar Testing, Presented at the SEM Annual Conference and Exposition, Springfield, MA, June 5, 2007.

5) Schmidt, Gilat, Walker, Seidt and Tyson, 3D Image Correlation Studies of Geometry and Material Property Effects During Split Hopkinson Bar Testing, Proceedings of the SEM Annual Conference and Exposition, Orlando, FL, June 2-4, 2008.

6) Seidt and Gilat, Characterization of 2024-T351 Aluminum for Dynamic Loading Applications, Proceedings of the SEM Annual Conference and Exposition, Orlando, FL, June 2-4, 2008.

7) Sunny, Lewandowski and Prakash, Effects of annealing and specimen geometry on dynamic compression of a Zr-based bulk metallic glass, J. Mater. Res., Vol. 22, No. 2, Feb 2007.

8) Sunny, Yuan, Lewandowski and Prakash, Effect of high strain rates on peak stress in a Zr-based bulk metallic glass, J. Appl. Phys. 104, 093522 (2008).

9) Kirugulige, Tippur and Denney, Measurement of Transient Deformations Using Digital Image Correlation Method and High-Speed Photography: Application to Dynamic Fracture, Applied Optics, Vol. 46, No. 22, August 1 2007.

10) M. S. Kirugulige and H. V. Tippur, Measurement of Fracture Parameters for a Mixed-Mode Crack Driven by Stress Waves using Image Correlation Technique and High-Speed Digital Photography, Strain, 2008.

11) Miller, Schreier and Reu, High-speed DIC Data Analysis From a Shaking Camera System, Proceedings of the SEM Annual Conference and Exposition, Orlando, FL, June 2-4, 2008.

12) Schmidt, T., Tyson, J., Some Common and Not So Common Applications of 3D Image Correlation, Proceedings of the GOM International User Meeting, Braunschweig, Germany, Sept 25, 2007.

13) Paulsen, Erne, et al, Wind Turbine Operational and Emergency Stop Measurements Using Point Tracking Videogrammetry, Proceedings of the SEM Annual Conference and Exposition, June 2009.